UNIVERSITY OF LEEDS

This is a repository copy of *Three-dimensional simulation of a secondary circular settling tank: flow pattern and sedimentation process*.

White Rose Research Online URL for this paper:
https://eprints.whiterose.ac.uk/182149/

Version: Accepted Version

Article:

de Almeida, RA, Rezende, RVDP, Mataczinski, AK et al. (4 more authors) (2020) Three-dimensional simulation of a secondary circular settling tank: flow pattern and sedimentation process. Brazilian Journal of Chemical Engineering, 37 (2). pp. 333-350. ISSN 0104-6632

https://doi.org/10.1007/s43153-020-00030-0

© 2021, Tsinghua University Press and Springer-Verlag GmbH Germany, part of Springer Nature. This is an author produced version of an article published in Building Simulation. Uploaded in accordance with the publisher's self-archiving policy.

Reuse

Items deposited in White Rose Research Online are protected by copyright, with all rights reserved unless indicated otherwise. They may be downloaded and/or printed for private study, or other acts as permitted by national copyright laws. The publisher or other rights holders may allow further reproduction and re-use of the full text version. This is indicated by the licence information on the White Rose Research Online record for the item.

Takedown

If you consider content in White Rose Research Online to be in breach of UK law, please notify us by emailing eprints@whiterose.ac.uk including the URL of the record and the reason for the withdrawal request.

White Rose
university consortium
Universities of Leeds, Sheffield & York

eprints@whiterose.ac.uk
https://eprints.whiterose.ac.uk/

Three-dimensional Simulation of a Secondary Circular Settling Tank: Flow Pattern and Sedimentation Process

Regiani Aparecida de Almeida[1*], *Ricardo Vicente de Paula Rezende*[1], *Andrey Kuiava Mataczinsk1*[1], *Amirul Islam Khan*[2], *Sandro Rogério Lautenschlager*[1]

1 Department of Civil Engineering, State University of Maringa, Paraná, Brazil

2 School of Civil Engineering, University of Leeds, Leeds LS2 9JT, United Kingdom

*Corresponding author: email: regy.al@gmail.com

Abstract

A secondary circular settling tank (SCST) with low hydraulic load was numerically analyzed for flow patterns, velocity field, turbulence interactions and sedimentation process. A transient, three-dimensional model with three phases was employed, clean water was considered as a continuous phase and the sludge as a dispersed phase, an air layer under atmospheric conditions was considered above the surface of the water to help establish an opening boundary condition at the top of the tank. The governing equations are solved~~Regarding the model solution~~, using the software ~~used was the~~ Ansys CFX commercial code. For the model validation, 2D and 3D approaches were analyzed and simulated flow patterns were compared with experimental data from the literature and then 3D approach was preferred for SCST simulation. The model was used to evaluate the flow in a pilot plant. The amount and location of sludge present in the SCST at the time was measured from its volumetric fraction. Higher velocity and turbulent kinetic energy generated by the inlet flow stream were observed at the bottom of the tank led to re-suspension of sludge particles. With the sludge outlet opened, after 30 minutes of simulation there was stabilization of the sludge and improvement in the settling process. With the sludge outlet closed, after 30 minutes of simulation there was an increase of approximately 1% of sludge concentrated at the bottom of the decanter. The results provided detailed insight into the hydrodynamic flow within the SCST and they will serve as a first step for further improvements in process efficiency.

Keywords: Secondary circular settling tank, Sedimentation, Computational fluid dynamics, Multiphase flow, Wastewater treatment.

Introduction

In the treatment of domestic and industrial wastewater it is essential to separate the treated wastewater from the biological sludge. The secondary settling tank (SST) is widely employed in the separation of solid and liquid phases in activated sludge processes treating domestic and industrial wastewater, such separation occurs by gravitational sedimentation (EKAMA *et al*., 1997). There are many important factors that directly affect the design of SST, such as local climatic conditions, variations in plant operating conditions, sedimentation velocity, geometric tank configurations and wastewater characteristics, such as density and viscosity (Clercq 2003, Bajcar, Steinman et al. 2011, Patziger 2016).

The flow inside a SST is quite complex, it consists of a variety of particles, with different sizes, shapes and densities, all under the effects of gravity, currents and turbulence, which may impair the deposition of particles in settling tanks (Al-Sammarraee, Chan et al. 2009). Further, complete understanding of the sedimentation process is dependent on tank geometry, operational parameters, physical, chemical and biological characteristics of the sludge. Hence, there is still great difficulty in completely modeling such sedimentation process. The existing computational methodology~~technology~~ only allows to work with a number of simplifications (Gong, Xanthos et al. 2011, Patziger 2016, Samstag, Ducoste et al. 2016).

The suspended solid particles in the influent settle to its bottom, separating the sludge from the remaining fluid, i.e., a mixture of solid particles in liquid establishing a multiphase liquid-solid flow. So in sedimentation process, a clear fluid will emerge at the top, while, at the bottom, the particles will slow down and form a sludge layer leaving the middle as a constant settling zone. Therefore, low concentration of suspended solids on the effluent leaving the SST can be an indicative of sedimentation efficiency.

The design of SCST can be done using some reference manual (WEF, 2005) however there are some assumptions that need to be considered. To overcome ~~overcame~~ some of ~~this~~ these assumptions we have used ~~it has been used the simulation in~~ Computational fluid dynamics (CFD), which has been shown to be a very useful tool in the prediction of multiphase flow patterns and process efficiency of a large number of water treatment processes (Wu 2010, Guo, Zhou et al. 2013, Li Lei and Ni 2014), e.g., in chemical and biological processes involving suspended growth nutrient removal and anaerobic digestion among others (Samstag, Ducoste et al. 2016). The separation process in settling tanks is an example of multiphase liquid-solid flow, where the suspended solids represent the dispersed phase in a continuous phase. Sometimes dispersed-phase volume fraction is designated as concentration (Crowe 2005).

When discussing the validation of CFD predictions, there has been a lack of experiments involving solid particles to corroborate with simulations (Lakghomi, Lawryshyn et al. 2015). Some relevant computational work on the efficiency of (SCST) has been published in the literature; however, since the settling process involves more than one phase, with great variability in the physical properties of the sludge, the complete modeling of the process is still quite difficult (Goula, Kostoglou et al. 2008, Al-Sammarraee, Chan et al. 2009). Most of the published numerical studies consider simplifications of the process with good approximations. Clercq (2003) covered several aspects regarding the modeling of a circular settler, using a two-dimensional model in a single phase, however, quite comprehensive, which considered the concentration of sludge as a passive scalar. It also considers the effects of the decanter bottom scraper (solids removal mechanism), changes in sludge rheology and sedimentation velocity. The passage of the scraper forced the lower flow discharge, neutralizing the gravitational force, after passage of the scraper only a certain concentration of dispersed solids in the main volume was observed, not a thick layer at the bottom of the sedimentation tank. The numerical work obtained good agreement when compared with the concentration of suspended solids obtained from experimental measurements.

Commented [AK1]: Please clarify what is meant by good

The performance and the central feed capacity in a SST are very sensitive ~~sensible~~ to the inflow intensity, due to the limited tank volume in where the kinetic energy will be dissipated. Therefore, changes in the tanks geometry or the addition of parts like baffles aim to dissipate this energy, reducing the turbulence in the fluid and avoiding particles re-suspension. Around the SST inflow entrance, turbulent currents cause variations in sludge concentration, which influence the depth of the thickening zone; hence, the efficiency of the sedimentation process (Bürger, Diehl et al. 2011). Patziger, Kainz et al. (2012), noted, when working with a single-phase two-dimensional model, non-Newtonian fluid and with a transport equation for suspended solids concentration, the~~at~~ low hydraulic load resulted in low turbulence level in the SST, providing better sludge settling and thickening as well as positively increasing sludge concentration.

Using a two dimensional (2D) model, Patziger (2016)~~, also with 2D model~~ studied two distinct sludge inflow configurations to determine changes in flow pattern and suspended solid concentration. It has been shown that by reducing the baffle height, there was a decrease in the high velocity uplift components (fluid velocity greater than sedimentation velocity). In this study a less extensive region of turbulence characterized by high values of turbulent kinetic energy is observed. This resulted in better sedimentation and thickening conditions therefore a more dense sludge layer at the bottom and characterizing cleaner water at the upper water outlet.

Although 2D models result in optimum results, certain three-dimensional features such as rotational structures in the flow cannot be captured by two-dimensional models (Kleine and Reddy 2006). In the literature there is a lack of numerical simulation of SCST using the three-dimensional approach. Thus, at the beginning of the present work, a comparison between two-dimensional and three-dimensional models for flow in an SCST is made.

In terms of validation and reliability of the results, qualitatively comparing the simulated results with similar case studies is already an indication that the results are physically coherent (Kleine and Reddy 2006); it is a way to guarantee the physical validation of the simulation. The validation of the mathematical model is a fundamental step of the numerical simulation. Thus, data from a literature work with images of the sludge flow pattern inside a circular decanter were used for the validation of the model presented in this work. Then, the Element Based Finite Volume Method (EbFVM) was used to visualize the flow pattern and quantify variables such as sludge velocity and concentration and consequently being able to improve the design of the SCST considered. In this work, the flow in a SCST, with low hydraulic load was studied from numerical CFD simulation with a multiphase, transient and three-dimensional model.

2. Methodology

2.1 Mathematical Model

We use ~~proposed~~ the mathematical model based on the Navier-Stokes equation of conservation of mass (1)~~(1)~~, of the amount of movement weighted by the Reynolds mean (RANS) (2)~~(2)~~ with the *k-ω* Shear Stress Transport model of turbulence (eq. (3)~~(3)~~-(4)~~(4)~~) was used.

2.2.1 Multiphase flow

The multiphase homogeneous model was employed for the simulations. In homogeneous multiphase flow, a common flow field, such as velocity and turbulence, is shared by all phases. The fluid is composed of three phases: air, water and sludge:

$$\frac{\partial}{\partial t}\left(\tilde{\rho}_{\alpha}\right)+\nabla\cdot\left(\tilde{\rho}_{\alpha}U_{\alpha}\right)=0 \quad \textbf{(1)}$$

Formatted: Font: (Default) Times New Roman, English (United States)

Formatted: Font: (Default) Times New Roman, English (United States)

Formatted: Font: (Default) Times New Roman, English (United States)

Formatted: Font: (Default) Times New Roman, English (United States)

$$\frac{\partial}{\partial t}\left(\tilde{\rho}_{\alpha}U_{\alpha}\right)+\nabla\cdot\left(\tilde{\rho}_{\alpha}U_{\alpha}\otimes U_{\alpha}\right)=\nabla\cdot\left(r_{\alpha}\bar{\mathbf{T}}_{\alpha}\right)+\tilde{\rho}_{\alpha}\mathbf{g}+\mathbf{M}_{\alpha}+\Gamma_{\alpha}U_{\alpha}, \qquad \textbf{(2)}$$

where r_{α} is the volumetric fraction of the α phase (water, sludge and air), $\tilde{\rho}_{\alpha}=r_{\alpha}\rho_{\alpha}$ is the effective density for the α-phase U_{α} is the velocity vector and $\bar{\mathbf{T}}_{\alpha}=-p\bar{\mathbf{I}}+2\mu\bar{\mathbf{D}}$ here p is the pressure, μ is the dynamic viscosity and $\bar{\mathbf{D}}$ is the tensor strain rate, $\bar{\mathbf{D}}=\left(\nabla U_{\alpha}+\nabla U_{\alpha}{}^{T}\right)$, $\mathbf{M}_{\alpha}$ is the interfacial force per unit volume and Γ_{α} is the mass transfer rate per unit volume.

2.2.2 Turbulence

The Reynolds number at the tank inlet is Re = 3000, which characterizes a turbulent flow. The k-ω based Shear-Stress-Transport (SST) model (Menter 1994) was employed in this work to determine the influence of turbulence in the settling processes. The model works by solving a turbulence frequency-based model k-ω at the wall and k-ε in the bulk of flow. The SST model introduce three new variables into the system of equations: turbulent kinetic energy k (per unit mass), the dissipation (per unit mass) of the kinetic energy ε and the turbulent frequency, ω. *T*he turbulent viscosity is linked to the turbulent kinetic energy and turbulent frequency in this way: $\mu_t=\rho_{\alpha}k/\omega$. A blending function ensures a smooth transition between the two models.

In equations (3)~~(3)~~ and (4)~~(4)~~, the stress tensor is computed from the eddy-viscosity concept, P_k's are the production rate of turbulence, the model constants are given by: $\beta'=0.09$, $\gamma=5/9$, $\beta=0.075$, $\sigma_k=\sigma_{\omega}=2.0$ (Wilcox 1986). The k-ω model accounts for the transport of the turbulent shear stress and gives highly accurate predictions of the onset and the amount of flow separation under adverse pressure gradients by the inclusion of transport effects into the formulation of the eddy-viscosity resulting in a major improvement, regarding flow separation predictions. The superior performance of this model has been demonstrated in a large number of validation studies presented in (Bardina, Huang et al. 1997).

Formatted: Font: (Default) Times New Roman, English (United States)

Formatted: Font: (Default) Times New Roman, English (United States)

$$\frac{\partial}{\partial t}\left(\tilde{\rho}_{\alpha}k_{\alpha}\right)+\nabla\cdot\left(\tilde{\rho}_{\alpha}U_{\alpha}k_{\alpha}\right)=\nabla\cdot\left(r_{\alpha}\left(\mu_{\alpha}+\frac{\mu_{t_{\alpha}}}{\sigma_k}\right)\nabla k_{\alpha}\right)+r_{\alpha}\left(P_{k\alpha}-\beta'\rho_{\alpha}k_{\alpha}\omega_{\alpha}\right)+P_{k\beta\alpha} \qquad (3)$$

$$\frac{\partial}{\partial t}\left(\tilde{\rho}_{\alpha}\omega_{\alpha}\right)+\nabla\cdot\left(\tilde{\rho}_{\alpha}U_{\alpha}\omega_{\alpha}\right)=\nabla\cdot\left(r_{\alpha}\left(\mu_{\alpha}+\frac{\mu_{t_{\alpha}}}{\sigma_{\omega}}\right)\nabla\omega_{\alpha}\right)+\frac{r_{\alpha}}{k_{\alpha}}\left(\gamma\omega_{\alpha}P_k-\beta\rho_{\alpha}k_{\alpha}\omega_{\alpha}^2\right)+P_{\omega\beta}, \qquad (4)$$

2.2.3 Terminal velocity of the particle

The separation of the solid particles from the fluid in the sedimentation processes occurs by gravity acting on the particles, which are a force that acts downwards, also, two other forces acts on the particles: the buoyancy force acting upwards and the drag force in the direction of the relative velocity between the fluid and the particle.

If the mixture velocity is greater than the terminal velocity of the particle, the re-suspension of the particles will occur. The particles will decay with speed v_t (Eq.(5)~~(5)~~) and particle drop time t_q is given as a function of the terminal velocity by: $t_q=H/v_t$, where H is the height of the tank, then, when a particle of size dp falls through a fluid, the free fall velocity can be estimated through the expression (Tchobanoglous, Burton et al. 2003):

$$v_t = \left(\frac{4 d_p g \left(\rho_p - \rho \right)}{3 \rho C_D} \right)^{1/2} \tag{5}$$

where ρ_p is the density of the particle, ρ is the density of the water and CD is the drag coefficient, which, for spherical particles in turbulent regions, is $C_D = 0.44$. In this work, d_p=1.0e^{-4} m, ρ_p=1400.0 kg m^{-3} and ρ = 997.0 kg m^{-3}.

2.2 Methodology for Model Validation

Initially two approaches were considered: two-dimensional and three-dimensional simulations were carried out with the purpose of verifying which approach would give better results when compared with experimental results. The two-dimensional approach computation time was approximately 48 hours and in the three-dimensional approach, this was approximately 200 hours.

Digital images of the experimental flow on SCST from the study of BAJCAR *et al*. (2011) were used. The images capture the whole flow field ~~on~~ in the space at once, which provides the ability to measure instantaneous velocities and analyze eventual spatial changes in the flow field through time. With the parameters and our geometry, a 2-D and 3-D mesh were created, as shown in Figure 1 and 2 respectively. The model considered has a length $L = 890\ mm$, which represent the radius of an analogous SCST, as can be seeing on the 3-D geometry in Figure 2. For the simulations, a three phase flow was considered: water, sludge and an air layer at the top of the tank as indicated in Figure 1. For the initialization of the simulations, the tank was filled with water. The volumetric flow rate in the system was 6.0 L min^{-1} with the sludge outlet permanently

Formatted: Font: (Default) Times New Roman, English (United States)

closed. According to Bajcar, Steinman et al. (2011), a material called "sludge" was created in the Ansys CFX software. Sludge, was considered with particle of 0.25 mm diameter (particle size large enough so that it is possible to clearly observe changes in suspension concentration after time intervals selected). With a density of 1450 kg m^{-3} and a viscosity of 0.8 kg m^{-1} s^{-1} this material was considered to be a dispersed fluid, with particles of diameter 0.25 mm, in water. The mesh with hexahedral elements containing 219829 elements and 144234 nodes was made in software ICEM-CFD 14.5.

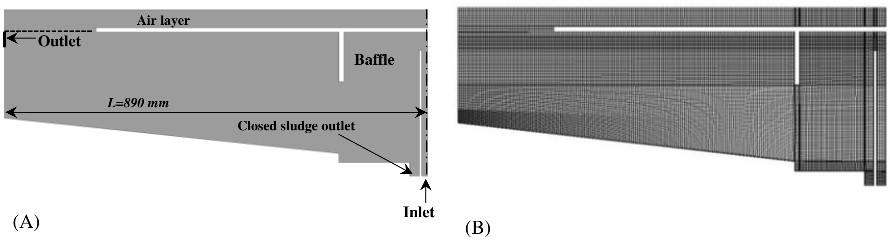

Figure 1: Two-dimensional geometry according to Bajcar et al. (2011) (A) with the entrance of sludge from the bottom (inlet), the outlet of water from the top tank (outlet) and the baffle at the top at the entrance; And (B) the hexahedral mesh employed.

For the three-dimensional simulation a circular tank was considered. The 2-D geometry of Figure 1 (A) was rotated 180 degrees around of vertical central symmetry axis. A mesh with tetrahedral elements was generated, as in Figure 2 (B).

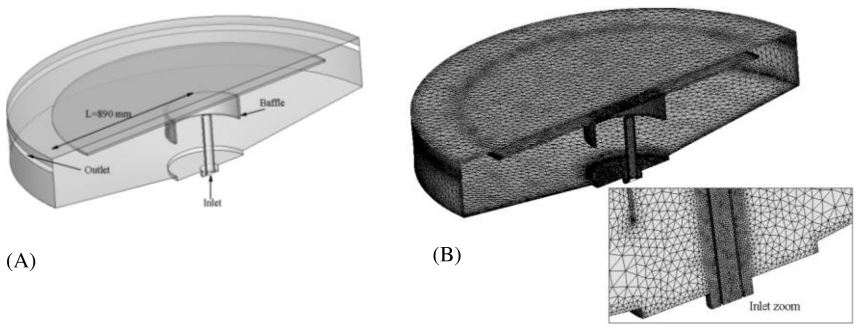

Figure 2: Three-dimensional geometry according to Bajcar et al. (2011) (A) with the entrance of sludge from the bottom (inlet), the outlet of water from the top tank (outlet) and the baffle at the top at the entrance; and (B) the Tetrahedral mesh employed.

2.2.1 Boundary Conditions

The boundary conditions at the inlet consists of a mass flow rate of 6.0 L min^{-1} and a sludge volumetric fraction of 1.5%. At the water exit, the flow was considered as opening boundary condition, but with zero sludge volume fraction. At the top of the tank it was considered a 0.05m layer with only air, with an opening boundary condition. This boundary condition can be used at boundaries in which the flow occurs in or out of the domain. The remaining boundaries of the domain were considered as walls with non-slip condition.

2.2.2 Validation Test: Two-dimensional Simulation

The comparisons of the results of the two-dimensional simulations obtained in this work, with the one from the literature, can be seen in Figure 3 and Figure 4. There is qualitative agreement between the flow patterns. In Figure 3 (B) and (D), as well as in (A) and (C), there is a significant density current at the bottom of the inner chamber. But in the ~~images~~ flow field obtained with computational simulation in this work, ~~the flow presents~~ shows larger areas of fluid recirculation at the bottom of the tank as shown in Figure 3 (B), (D). In the experimental work the flow is more regular than when compared to the computational simulation. Such a difference may be due to the three-dimensional nature of the flow.

Commented [AK2]: If quantitative, please show graphs

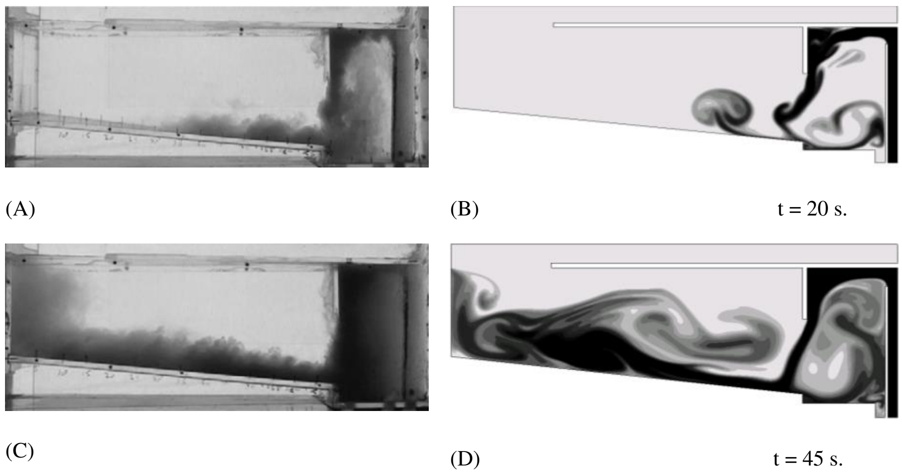

Figure 3: Sequence of images of suspension flow obtained from Bajcar et al. (2011) (A) e (C); Contour maps colored by the volumetric fraction of sludge, obtained in this work with the two-dimensional approach (B) e (D).

2.2.2 Validation Test: Three-dimensional Simulation

The mathematical model and boundary ~~contour~~ conditions described above were employed to obtain 3-D results with the mesh shown in Figure 2 (B). The comparative results with the same experimental images of Figure 3 (A) and (C) are done with the results of the 3D simulation in Figure 4, in which a central cutting plane to the geometry was colored with the variable volumetric fraction of sludge in the same color scale described in Bajcar et al. (2011). Comparing the images (A) and (B) of Figure 4, it is observed that in the first 20s of simulation, there are some differences in the amount of sludge present at the bottom of the settler, but a good agreement was obtained on the flow pattern. At 45 s, a larger sludge spread is observed in the region below the baffle Figure 4 (D) when compared to Figure 4 (C). Bajcar et al. (2011) measured ~~got that~~ the fluid flow along the bottom tank and obtained a flow ~~have~~ velocity of about 4 cm/s. ~~and~~ Similarly along the outer wall of the settling tank (left side of images in Figure 4(C)) ~~and reaches it with the~~ he measured a velocity of approx. 2.5 cm s^{-1}. In our~~this~~ study, the velocity at the bottom tank was about 3.7 cm s^{-1} and the outer wall of the settling tank (left side of images in Figure 4(D)) the velocity was about 1.7cm s^{-1}.

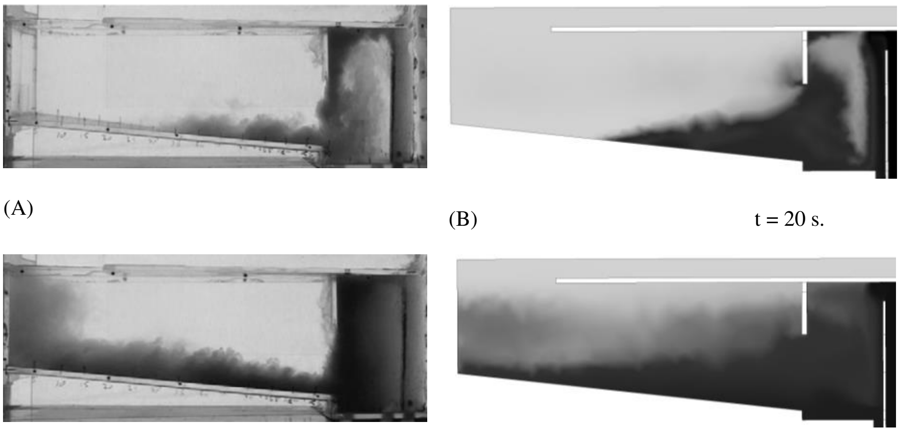

(A) (B) t = 20 s.

(C) (D) t = 45 s.

Figure 4: Comparative images between the concentration of sludge in the experimental work of Bajcar et al. (2011) at approximately t = 20s and t = 45s of operation (A) and (C) respectively; and the volume fraction of sludge at t = 20s and t = 45s of 3D simulation, (B) and (D), respectively.

Both approaches 2D and 3D showed agreement with the chosen experimental case. However, when considering the 3D domain, the fluid waves have more space to dissipate, so they are expected to be lower and last for less time, thus generating smaller oscillations with less intensity. Thus, even with high computational

Commented [AK3]: Do you mean boundary conditions??

Commented [AK4]: Clarify good in terms of numbers. How do you know it is good, are the predictions within few percent of the measurements?

Commented [AK5]: Need reference, or mention about vortex stretching which doesn't exist in 2D flow time, the 3D case is more adequate for the sludge distribution inside the settling tank and was chosen to simulate a SCST pilot plant with similar operating conditions.

2.3 Simulation of the flow pattern for a new SCST

2.3.1 Geometry

The new SCST tank has 2m of height and 1m of diameter and total volume 1.57m². The mass transport, as well as the regions of the computational domain of water, sludge inlet, sludge outlet and clean water outlet is indicated in Figure 5 (A), where Q and QRS are inflow rate and return sludge flow rate in m^3s^{-1} respectively. Views of the project detail plane as well as the dimensions of the tank under study are shown in Figure 6. For the CFD simulations, from the detailed design (Figure 6 (A)) some geometric simplifications must be considered (Figure 6 (B)): the internal scrapers responsible for scraping the sludge from the bottom of the tank were removed, as well as parts of the fixation of inlet pipe and baffle.

2.3.2 Mesh independence

In order to test the independence of the mesh employed, four meshes with increasing refinement on the computational domain were considered. Simulations preliminaries considering steady state regime with just clean water on the tank were made for each mesh using the boundary conditions of Table 2. Meshes with tetrahedral elements and with different densities were tested. For each mesh, by setting the inlet flow rate, the outlet velocity was measured and compared to the measured outlet velocity experimentally. The values obtained for each mesh can be compared from Table 1.

From the mesh number 02 onwards, the velocity field~~s~~ practically did not vary significantly ~~present modifications~~ when compared with the same field~~s~~ obtained with the meshes 03 and 04. ~~And t~~The velocity values measured at~~in~~ the outlet did not suffer variations as well, as shown in Table 1. Thus, it was opted for ~~to~~ use ~~mesh 02~~ for all the multiphase transient simulation containing water and sludge.

Table 1: Calculated and simulated velocity values at the clean water outlet (tank top) for the four test meshes.

		Number of elements (million)	Theoretical	Simulation	Error %
Top outlet velocity [m/s]	Mesh 01	1.50	0,0103	0,0111	7.7
	Mesh 02	1.87		0,0110	6.7
	Mesh 03	5.39		0,0110	6.7
	Mesh 04	7.16		0,0110	6.7

With that information, the mesh employed on the considered geometry consists of approximately 1.87 million tetrahedral elements and the distribution of such elements can be seen in Figure 5 (B).

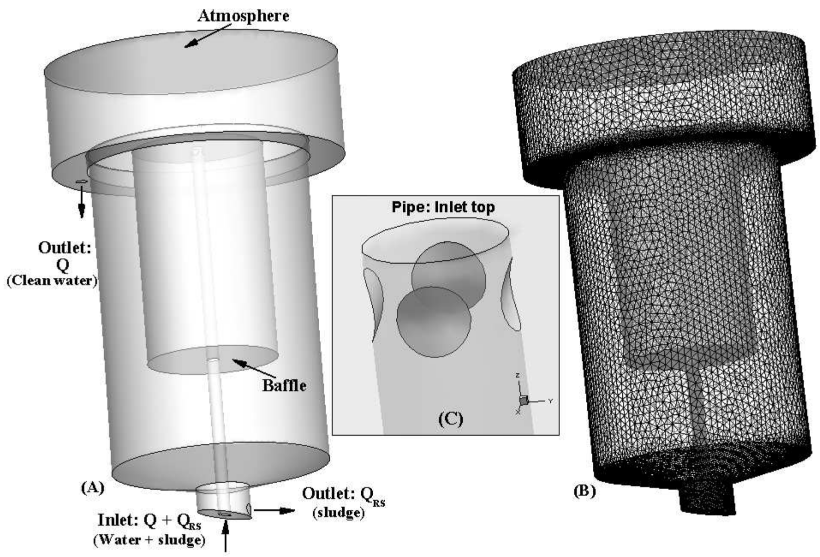

Figure 5: Three-dimensional geometry with the inlet and outlet regions (A); And tetrahedron mesh over the computational domain (B); Zoom of holes at inlet pipe top (C).

2.3.3 Boundary Conditions

An “inlet” contour boundary condition was employed at the sludge inlet, under a flow rate of 3 m^3 day^{-1}. The outlets boundary conditions "opening" was specified in the outlet of clean water and in the lower sludge outlet, in those boundaries of the computational domain the “Bulk mass flow rate” option was established. The

Commented [AK6]: ??

specific values and their respective units used in the simulation are shown in Table 2. The recirculation flow rate was considered constant.

Table 2: Values specified in the boundary conditions.

Inlet flow rate [kg s^{-1}]	0.034
Recirculation flow rate [kg s^{-1}]	0.013
Turbulence at the inlet [%]	1.0
Volumetric fraction of sludge in the inlet [-]	0.1
Turbulence at the Sludge outlet [%]	1.0
Sludge outlet flow rate [kg s^{-1}]	0.0195
Turbulence at the sludge outlet [%]	5.0
Turbulence at the outlet of clean water [%]	1.0

A common problem in SCST is the effluent inlet geometry, directly responsible for the increased turbulence in the system (Patziger 2016). From the use of a baffle it is possible to redirect the flow of liquid to reduce the formation of instabilities in the velocity field caused by the inlet kinetic energy and to reduce the sludge re-suspension. For the geometry studied here, the effluent enters in the tank through a central pipe with circular holes at the top (Figure 5 (C)), those four holes were set as the inlet boundary condition, also a baffle of 0.6 m in diameter by 1.0 m height was used, according to Figure 6 (B). On the walls of the baffle, as well as on the walls of the tank, boundary conditions of “no slip” were applied.

2.3.3 Numerical details

The tank filled with water was considered as initial condition, the initial time step for the discretization of the differential equations in time was $\Delta t = 0.01$s for the first 20s of simulation, from there the system remained stable with residual error down to 10^{-5}, then to decrease the computational time was considered $\Delta t = 0.1$s and for all variables the residual error remained below 10^{-4}.

As for the numerical schemes employed, high resolution advection scheme was used and for transient scheme a second order Backward Euler scheme was employed.

All the simulations were performed~~Was employed a~~ on a workstation with 64-bit operating system, ~~system with~~ four processors running at ~~with~~ 2.26 GHz and ~~,~~ 16GB of memory (RAM). ~~and 64-bit operating system to calculate the solution.~~

2.3.4 Initial Conditions

For the transient simulation, the SCST was filled with clean water up to 1.58m height with an air layer of 0.42m above this specified height. Such condition is given by equation (6)~~(6)~~ and indicated in Figure 6 (B):

Formatted: Font: (Default) Times New Roman, English (United States)

$$H(z)=\begin{cases} Water_{vf}=1, \ if & 0\le z\le 1.58 \\ Water_{vf}=0 \ if & 1.58\le z\le 2.0 \end{cases} \qquad (6)$$

where $Water_{vf}$ is the volumetric fraction of water and z is the Cartesian axis in which the height of the tank is located. Spatial initial condition: null pressure and null Cartesian velocity components.

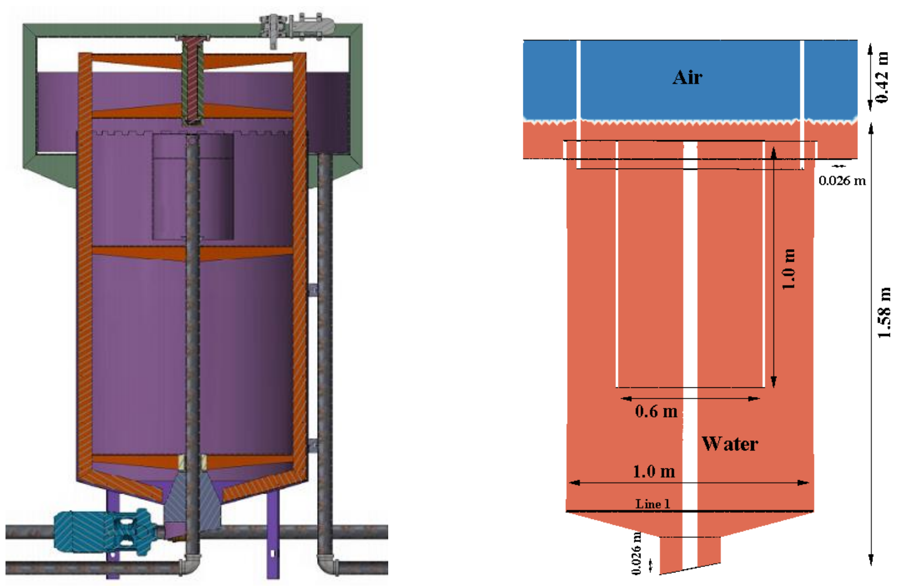

(A) (B)

Figure 6: Views of the central plane of settling tank; A) Detailed design of the original settling tank geometry; B) CFD design of settling tank with initial condition for transient simulation and geometric dimensions.

3. Results and discussion

3.1 Velocity field

In the homogeneous model employed in this work, the water velocity field as well as the dispersed solids velocity field is the same. However, to recover information about water velocity and sludge velocity separately, one can analyze the variable superficial velocity. The superficial velocity is important in the representation of phenomena typical of multiphase flows; it is defined as the fluid volume fraction multiplied by the fluid velocity. So, this variable is used in vector plots at multiphase flow, as we will only see a vector where a significant amount of that phase exists. A cut plane colored by the sludge superficial velocity and overlapped~~ing~~ by ~~your~~ streamlines and sludge superficial velocity vectors is shown at Figure 7, it can be seen that there is a significant amount of sludge in the bottom region, higher sludge velocity at the bottom of the tank and that there is much fluid recirculation throughout the tank interior.

The fluid entering the tank at reaches its bottom forming areas of recirculation near the outlet of the sludge, Figure 7 (A)-(C). This fluid returns upward with sufficient velocity so that by finding the inclined bottom walls of the tank and the side walls form other small recirculation regions. Then part of the fluid is drawn back for inside the baffle, Figure 7 (B), where, on the top of the baffle, there is a fresh fluid encounter with the upward current and part of this mixture descends again around the central tube toward the bottom of the tank.

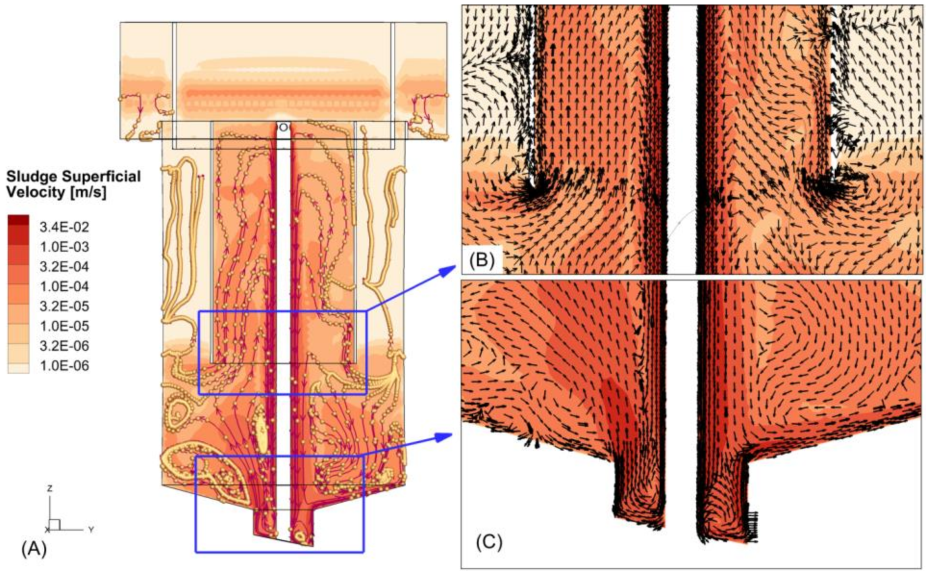

Figure 7: Central cut plane colored by sludge superficial velocity overlapping with streamlines (A); (B) region of the baffle outlet colored by sludge superficial velocity overlapping with the superficial velocity of sludge vectors; (C) region of the tank bottom (sludge outlet) colored by superficial velocity of sludge overlapping with the superficial velocity of sludge vectors.

The velocity of the jet formed at the inlet from the holes at the top of the tank is high, around 0.1 m / s and continues high around the inlet tube until it reaches the bottom, where there are small and tortuous recirculation zones. As can be seen from figure 7 and 8, the superficial velocity of the water is greater than the superficial velocity of the sludge by an order of magnitude. At very low velocity the fluid travels down smaller paths losing energy and the particles settle. On the other hand, for very high velocity the particles are drawn by the continuous phase, towards the exit. The equation (5)~~(5)~~ gives an idea of the magnitude of the terminal velocity of the particle.

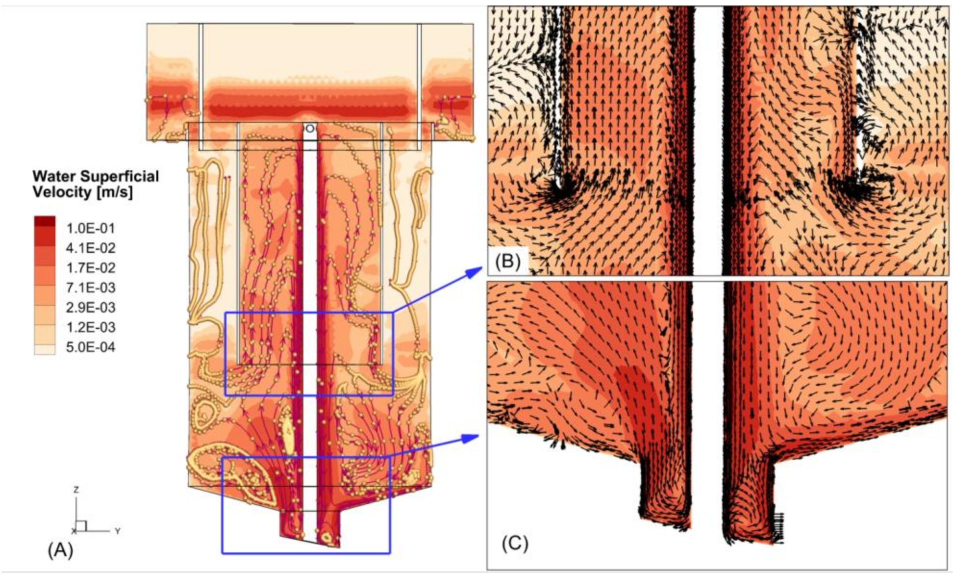

Figure 8: Central cut plane colored by water superficial velocity with streamlines overlapping (A); (B) the region of the sludge inlet colored by superficial velocity of water and vectors; (C) region of the tank bottom colored by superficial velocity of water and vectors.

Then, with the equation (5)~~(5)~~ we got v_t = 0.034 m/s. In Figure 9 it is possible to compare the magnitude of the calculated fluid velocity *v,* in a few instants of time, in a sampling line, indicated in Figure 6

Formatted: Font: (Default) Times New Roman, 10 pt

Formatted: Font: (Default) Times New Roman, 10 pt, Not Bold, Check spelling and grammar

Formatted: Font: (Default) Times New Roman, 10 pt

Formatted: Font: (Default) Times New Roman, English (United States)

Formatted: Font: (Default) Times New Roman, Not Bold, English (United States), Check spelling and grammar

Formatted: Font: (Default) Times New Roman, English (United States)

(B) as line 1. The line is located horizontally, in the center, at the bottom of the tank (0.01m from the bottom). It can be observed that at the bottom of the tank there is high fluid velocity mainly in the center around the inlet pipe (0.12 m/s), the dotted line indicate in the graph the particle terminal velocity, which gives the dimension of how much the terminal velocity v_t is smaller than surrounding fluid velocity. It can be stated that the particles settled at the center and bottom of the tank will undergo re-suspension because in this region $v > v_t$. In Figure 9 it can be observed that the velocity of the fluid in the center of the tank increases until the time t = 20 min. At t = 30 min and t = 36 min the fluid velocity at the bottom of the tank in its central region decreases. In the region near the walls at the bottom of the tank, $v \le v_t$. This indicates that in this region, particles are less likely to undergo re-suspension.

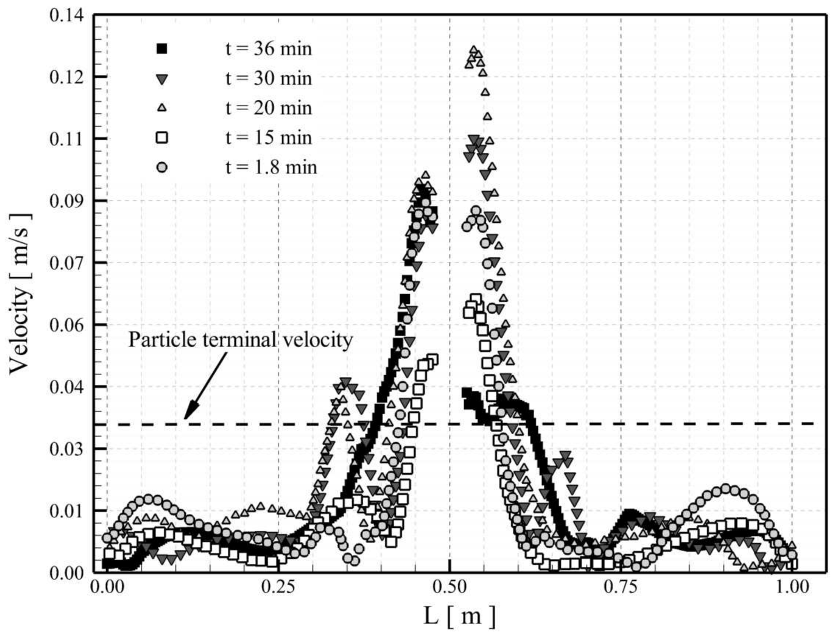

Figure 9: Magnitude of the velocity variable evaluated on line 1 located at the central plane at the bottom of the tank, evolution over time.

The contour maps of Figure 7 show the velocity field ranging from 0 m/s to 0.034 m/s at a central plane of the geometry. The water and sludge mixture runs a distance of 1.74m from the inlet holes at the top of the tank until it reaches the bottom of the tank in the region of the sludge outlet. Thus, when it reaches the bottom and as discussed above, it can be seen that the higher velocity zones are around the central inlet pipe. Then, it can be said that inlet jet causes disturbances in the bottom of the tank. This makes its performance difficult. When the fluid recirculates, irregular velocity regions are formed, still with high speed entering the baffle. From the moment that fluid reaches the bottom of the tank, over time (30min and 36min), there is a small decrease in the velocity as in Figure 9, around the bottom of the tank there are oscillations of fluid velocity.

In Figure 8, we also note that at a height of 0.65 m, the superficial velocity of water decreases to the order of $5e^{-4}$ m/s in the region outside the baffle (from the region above the baffle outlet). In this region the superficial velocity of the sludge is around $1e^{-6}$ m/s. It can be said then that in the upper part of the tank, above the baffle outlet, there is little possibility of particle re-suspension.

3.2 Turbulence

The magnitude of turbulent kinetic energy remains low inside the tank. The flow starts with the formation of a jet of fluid denser than water and formation of initial instabilities near the central inlet tube, as can be seen in Figure 11 from t=2min. When the fluid with sediment touches the bottom of the tank, currents are formed in which turbulent instabilities are observed. The turbulent kinetic energy was calculated on a line of sampling points (Figure 7(B) - Line 1). It can be observed in the Figure 10 that with the increase of the time, until t=30min, there is turbulence increase at the bottom of the tank. As observed in the previous section, the fluid that reaches the bottom of the tank presents high velocity, being able to load particles to regions closer to the baffle impacting the clarified quality. But at t=36 min, it is observed that there is a decrease in the value of the turbulent kinetic energy, around 0.25 cm^2/s^2, this indicates that with the increase in time, particles can decant more easily. This fact can be observed when analyzing Figure 12 at t = 36 min, that is, there is a higher concentration of sludge at the bottom of the sedimentation tank, around 1.4%. In general the turbulent kinetic energy in the liquid phase varied very little, from 0-0.5 cm²/s², being that the maximum was observed around the central pipe of inlet. And the highest values (about 40 cm²/s²) were observed in the air layer that was considered above the liquid phase as already shown in Figure 7 (B).

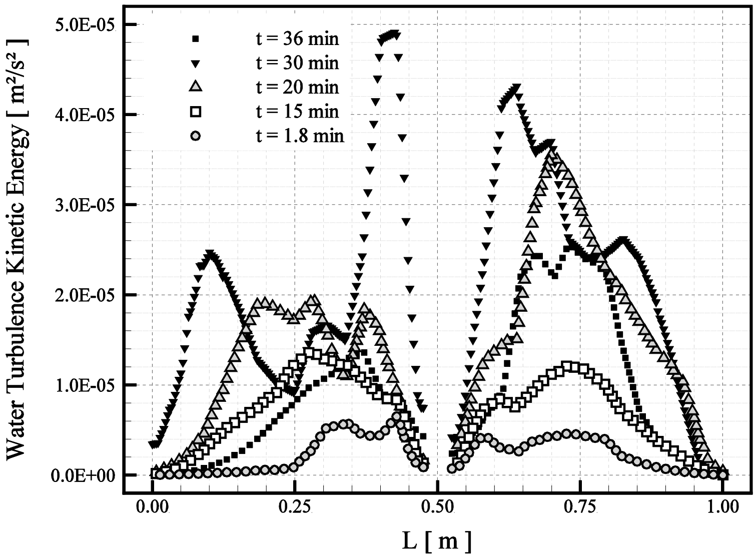

Figure 10: Turbulent kinetic energy evaluated on line 1 located in the central plane at the bottom of the tank.

3.3 Concentration of suspended solids

In the present study the scraper was not considered at the bottom of the tank, so the sludge was able to build up. In the first 36 minutes of simulation the sludge outlet was kept open. After this time it was closed and simulated another 24 minutes.

In Figure 11 and Figure 12, the increase in the height of the concentrated sludge layer is observed over time, that is, the evolution of the volume fraction of sludge with time in the tank. Therefore, it is possible to visualize the sedimentation process. It is observed that at the initial time t=20s, the jet with sludge and water is beginning its development, at t=2min the portion of fluid containing 0.6% of sludge is deposited in the bottom. And in the following instants the volume of the tank occupied with such amount of sludge increases.

At t=20 min, about 0.8% sludge portion reaches approximately the height of the baffle outlet, even this percentage of sludge enters the interior of the baffle.

At t=36min it is already possible to observe 1.2% of sludge fraction accumulated in a thinner layer at the bottom of the tank. This indicates that in 36min there is greater accumulation of sludge at the bottom of the tank. This fact is in agreement with the data obtained in Figures 9 and 10, with less magnitude of velocity and less turbulence at the bottom of the decanter, there is less re-suspension of particles and a greater amount of sludge accumulates at the bottom of the tank.

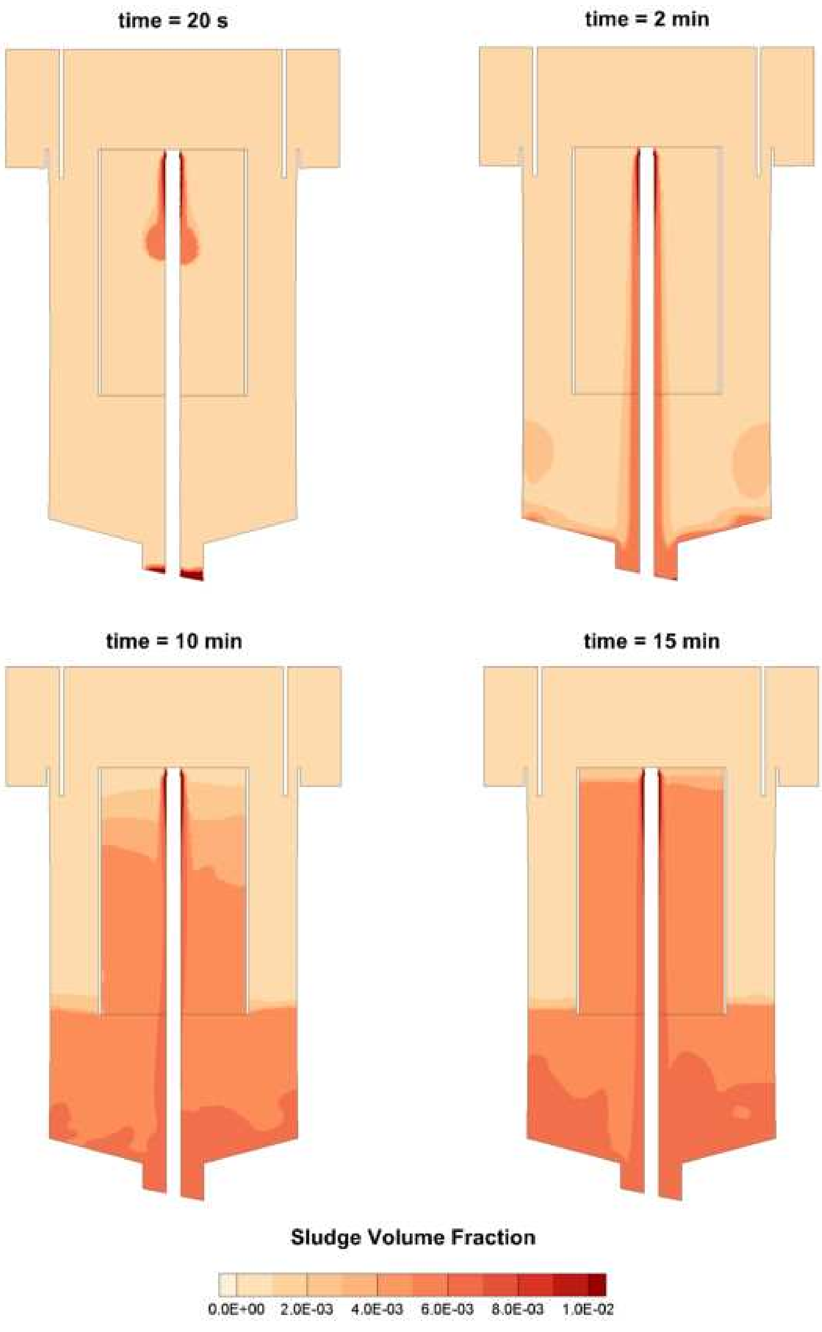

389

390 **Figura 11: Sludge volume fraction in the initial instants of the simulation with sludge outlet opened.**

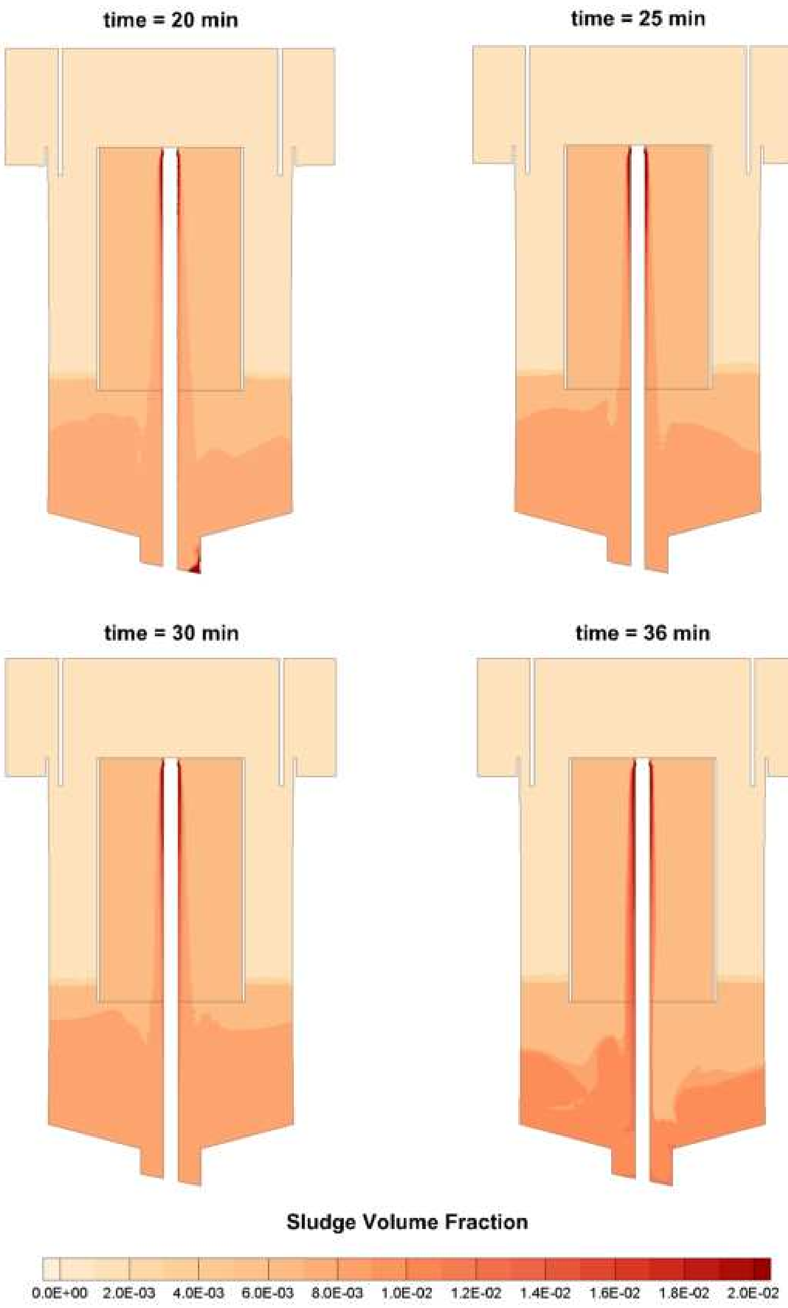

Figura 12: Sludge volume fraction in the final moments of the simulation with sludge outlet opened.

The operation of the decanter was also simulated with the outlet of sludge closed, to observe the denser and rich microorganism sludge depositing in the bottom of the tank, then the microorganisms that grow in the system need to be discarded and posteriorly the sludge outlet must be reopened. The heavier sludge is scraped to a central well; the scraper system was not simulated in this work. After 36 minutes of simulation, the sludge outlet was closed and the most intensive sedimentation process could be observed.

As expected, the increase of concentrated sludge at the bottom of the decanter is observed at t = 60 min (2% of sludge) as seen in Figure 13. To illustrate the increase of settled sludge particles in units of mass concentration, see Figure 14.

Na opening boundary conditian was chosen for the sludge outlet boundary condition and also for the clean water outlet boundary condition because it was numerically more stable. An opening condition can be used at a boundary where the flow is into or out of the domain. All of the fluid might flow into the domain at the opening, or all of the fluid might flow out of the domain, or a mixture of the two might occur. For this reason, it was observed an increase in the volume fraction of sludge very close to the sludge outlet in some stages of the simulation, as in t=10min, t=15min and t=20min in Figure 13 and on the chart t=20min in Figure 14.

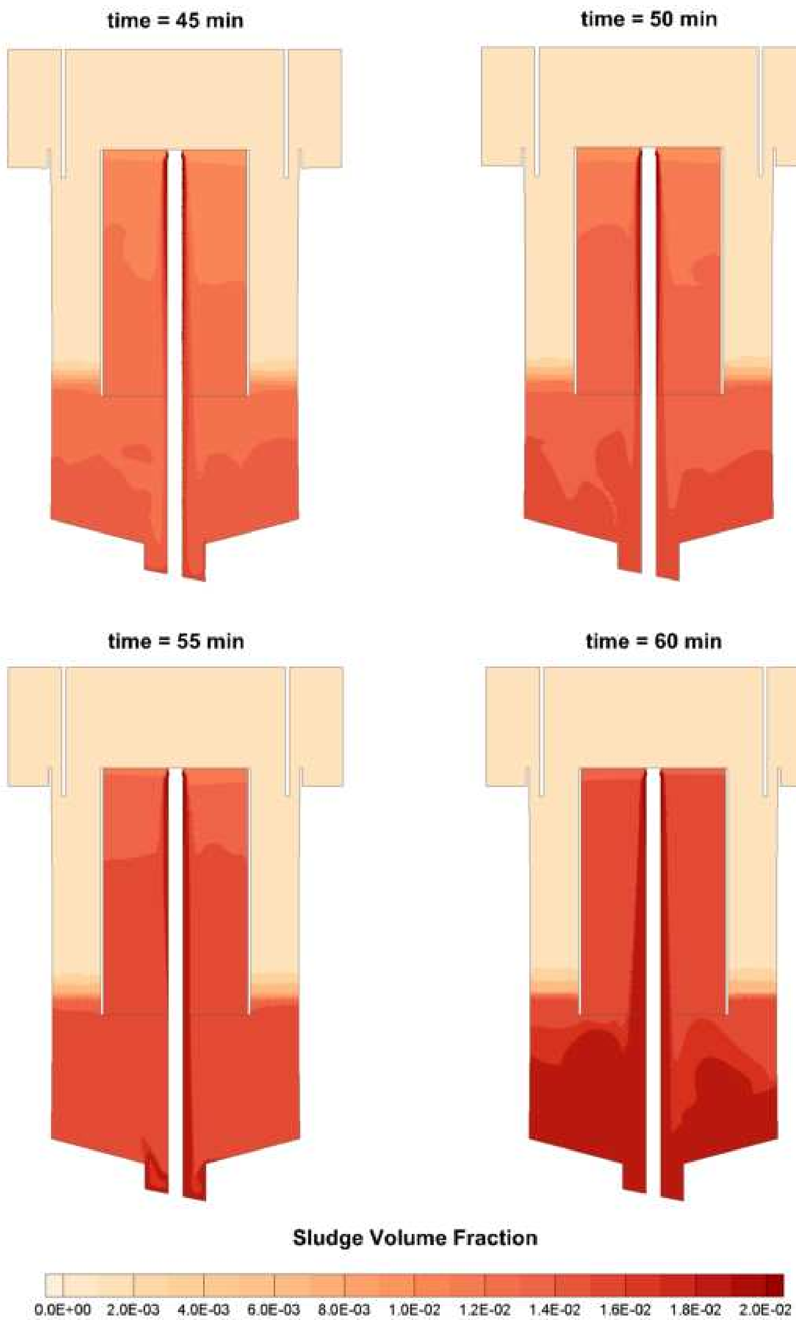

Figura 13: Sludge volume fraction in the final moments of the simulation with sludge outlet closed.

To evaluate the magnitude of the sludge concentration at specific sites of the tank, two sampling lines were considered inside the tank, both in the vertical position (parallel to the z-axis), the first, **line 2** is situated in the central plane ($y \times z$) at 0.02m from the sludge outlet. The second line, **line 3** is situated in the center plane ($x \times z$) at 0.09m from the side wall of the tank.

As can be seen in Figure 14, at the beginning of the simulation, at t=10min at a height of 1.5m there is a sludge concentration of approximately 0.25g/l on line 2 near the center of the tank and such concentration increases as the height decreases. At the bottom of the tank near the outlet of sludge on line 2, there is concentration of 2.8g/l. However, on the line 3 situated closest to the wall, it is observed an increase in the concentration of sludge from a height of 0.5m with 2.0g/l and of 2.7g/l at the bottom of the tank. In line 2 (near the center) there is a significant concentration of 1.5 m, since line 2 is located in the region of the inside of the baffle where there is sludge recirculation and in line 3 (near the wall) a significant concentration of sludge is observed only from 0.5m in height. In both lines there is greater concentration in the bottom of the tank.

At t=36min, concentration at the bottom of the tank is observed around 11.5g/l and 10.4g/l in lines 2 and 3 respectively. These values in their magnitude are in agreement with the work of (Patziger, Kainz et al. 2012). And after the sludge exit is closed it is observed at the bottom of the tank an increase of approximately 40% of sludge in both sampling lines.

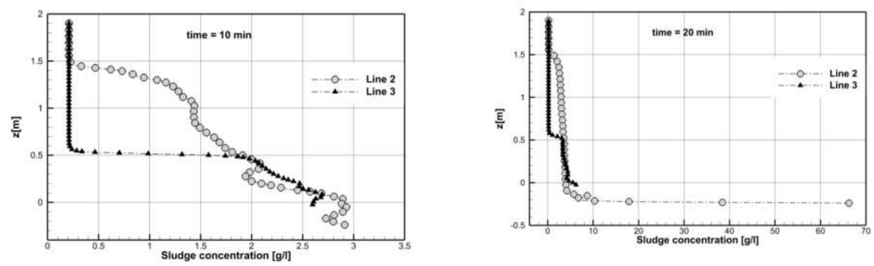

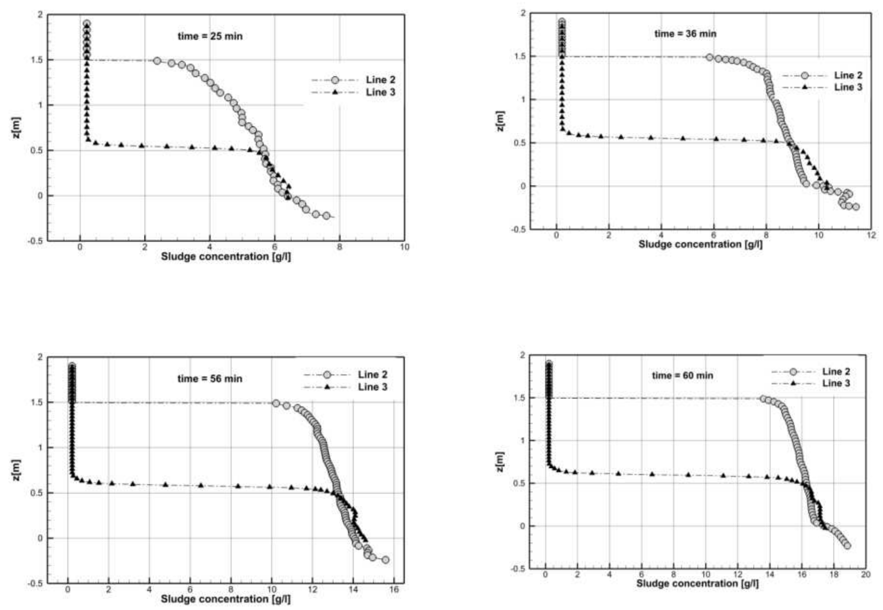

Figure 14: SS concentrations in line 1 and line 2, representative vertical profiles of the SCST

An isosurface is a surface of constant value for a given variable. That is, a three-dimensional surface that defines a single magnitude of a flow variable such as volume fraction. The Figure 15 shows the chaotic nature of the fluid's behavior in the tank in t=36min and t=60min. The rapid increase of sludge particles is observed when the sludge outlet is closed t=60min. When the fluid with higher density (water + sludge) enters with high velocity in the tank containing water, this is pushed up by the fluid recirculating into the baffle and reaches the walls of the baffle as it is possible to visualize from the isosurface with 1.1% sludge volume fraction at t = 60 min for example.

The fluid with larger volumetric fractions of sludge that are observed at the bottom of the tank also has many small recirculation zones, both at t=36min and at t = 60min, this may cause resuspension of sludge particles. To reduce the disturbances in the bottom of the tank it would have to have a larger diameter and lower height, like this, there would be greater area in the bottom so that the high velocity observed in the center could decrease.

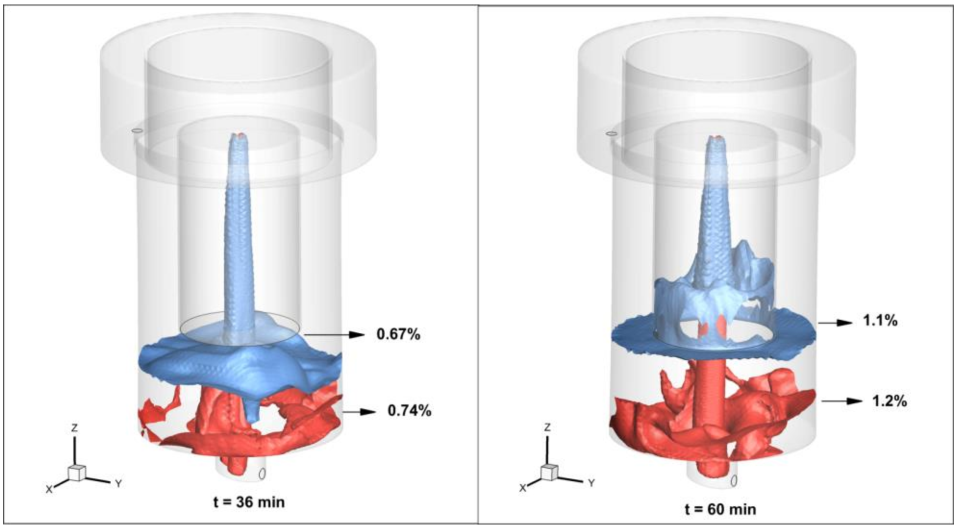

Figure 15: Sludge volume fraction by isosurfaces with two different values for t=36min and t=60min respectively.

4. Conclusions

A three-dimensional model in a three-phase transient regime was used to obtain information about the flow behavior in an SCST.

Comparisons between two-dimensional and three-dimensional simulations of an experimental SCST case from the literature showed that the 2-D mathematical model captures flow patterns, but with the 3-D model there is better agreement when comparing the sludge volume fractions in the tanks.

With the sludge outlet open, the velocity field shows that even working with low hydraulic loading will re-suspend the particles accumulated at the bottom of the tank because this is a region of high velocity and turbulence. The turbulent kinetic energy and the velocity at the bottom of the tank are smaller after 30 minutes of simulation. Also, analysis of the fields of sludge volume fractions display the water-sludge interface and it is observed that in the final time instants of the simulation the decanting process is more stable, there is a layer of higher concentration of particles at the bottom of the tank.

With the sludge outlet closed, as expected, an increase in the sludge volume fraction was observed, consequently in its concentration.

The model proved to be numerically stable and able to predict the distribution of sludge in the tank. The computation time for one hour of simulation was 180 days. The present study is the first step in the understanding of the hydrodynamic parameters involved in the optimization of a pilot plant of a SCST, from here, the model may be employed in future works to test other operating conditions, geometric modifications and the simulation time should be increased.

Acknowledgements

CNPq, CAPES, Fundação Araucaria, FINEP.

References

Al-Sammarraee, M., A. Chan, S. M. Salim and Mahabaleswar (2009). "Large-eddy simulations of particle sedimentation in a longitudinal sedimentation basin of a water treatment plant. Part I : Particle settling performance." Chemical Engineering Journal **152**: 7.

Bajcar, T., F. Steinman, B. Sirok and T. Preseren (2011). "Sedimentation efficiency of two continuously operating circular settling tanks with different inlet - and outlet arrangements." Chemical Engineering Journal **178**: 8.

Bardina, J. E., P. G. Huang and T. J. Coakley (1997). Turbulence Modeling Validation Testing and Development. NASA Technical Memorandum 110446.

Bürger, R., S. Diehl and I. Nopens (2011). "A consistent modelling methodology for secondary settling tanks in wastewater treatment." Water Research **45**(6): 2247-2260.

Clercq, B. D. (2003). Computational Fluid Dynamics Of Settling Tanks: Devevelopment of Experiments and Rheological, Settling, and Scraper Submodels., University of Gent.

Crowe, C. T. (2005). Multiphase Flow Handbook, Taylor & Francis Group - CRC Press.

Gong, M., S. Xanthos, K. Ramalingam, J. Fillos, K. Beckmann, A. Deur and J. A. McCorquodale (2011). "Development of a flocculation sub-model for a 3-D CFD model based on rectangular settling tanks." Water Science & Technology **9**: 8.

Goula, A. M., M. Kostoglou, T. D. Karapantsios and A. I. Zouboulis (2008). "A CFD methodology for the design of sedimentation tanks in potable water treatment." Chemical Engineering Journal **140**(1): 110-121.

Guo, X., X. Zhou, Q. Chen and J. Liu (2013). "Flow field and dissolved oxygen distributions in the outer channel of the Orbal oxidation ditch by monitor and CFD simulation." J Environ Sci (China) **25**(4): 645-651.

Kleine, D. and B. D. Reddy (2006). Finite Element Simulation Of Unsteady Flows In Secundary Settling Tanks. Fifth International Conference on CFD in the Process Industries. CSIRO, Melbourne, Australia**:** 6.

Lakghomi, B., Y. Lawryshyn and R. Hofmann (2015). "Evaluation of flow hydrodynamics in a pilot-scale dissolved air flotation tank: a comparison between CFD and experimental measurements." Water Science et Technology **72**: 7.

Li Lei and J. Ni (2014). "Three-dimensional three phase model for simulation of hydrodinamics, oxygen mas transfer, carbon oxidation, nitrificationn and denitrification in a oxidation ditch." Water Research: 14.

Menter, F. R. (1994). Two-equation eddy-viscosity turbulence models for engineering applications. AIAA-Journal.

Patziger, M. (2016). "Computational fluid dynamics investigationof shallow circular secondary settling tanks: Inlet geometry and performance indicators." Chemical Engineering Research and Design: 10.

Patziger, M., H. Kainz, M. Hunze and J. Józsa (2012). "Influence of secondary settling tank performance on suspended solids mass balance in activated sludge systems." Water Research **46**(7): 2415-2424.

Patziger, M., H. Kainz, M. Hunze and J. Józsa (2012). "Influence of Secondary Settling Tank Performance on Suspended Solids Mass Balance in Activated Sludge Systems." Water Research **46**: 11.

Samstag, R. W., J. J. Ducoste, A. Griborio, I. Nopens, D. J. Batstone, J. D. Wicks, S. Saunders, E. A. Wicklein, G. Kenny and J. Laurent (2016). "CFD for wastewater treatment: an overview." Water Science et Technology **74 (3)**: 14.

Tchobanoglous, G., F. L. Burton and H. D. Stensel (2003). Wastewater engineering : treatment and reuse/ Metcalf&Eddy,Inc.

, Fourth edition / revised by George Tchobanoglous, Franklin L. Burton, H. David Stensel. Boston : McGraw-Hill, [2003] ©2003.

Wilcox, D. C. (1986). Multiscale model for turbulent flows. In AIAA 24th Aerospace Sciences Meeting. American Institute of Aeronautics and Astronautics.

Wu, B. (2010). "CFD simulation of mixing in egg-shaped anaerobic digesters." Water Research **44**(5): 1507-1519.